Particle motions caused by seismic interface waves

Jens M. Hovem,
jmhovem@gmail.com

37th Scandinavian Symposium on Physical Acoustics
Geilo 2nd - 5th February 2014

Abstract

Particle motion sensitivity has shown to be important for fish responding to low frequency anthropogenic such as sounds generated by piling and explosions. The purpose of this article is to discuss the particle motions of seismic interface waves generated by low frequency sources close to solid rigid bottoms. In such cases, interface waves, of the type known as ground roll, or Rayleigh, Stoneley and Scholte waves, may be excited. The interface waves are transversal waves with slow propagation speed and characterized with large particle movements, particularity in the vertical direction. The waves decay exponentially with distance from the bottom and the sea bottom absorption causes the waves to decay relative fast with range and frequency. The interface waves may be important to include in the discussion when studying impact of low frequency anthropogenic noise at generated by relative low frequencies, for instance by piling and explosion and other subsea construction works.

1 Introduction

Particle motion sensitivity has shown to be important for fish responding to low frequency anthropogenic such as sounds generated by piling and explosions (Tasker et al. 2010). It is therefore surprising that studies of the impact of sounds generated by anthropogenic activities upon fish and invertebrates have usually focused on propagated sound pressure, rather than particle motion, see Popper, and Hastings (2009) for a summary and overview.

Normally the sound pressure and particle velocity are simply related by a constant; the specific acoustic impedance $Z=\rho c$, i.e. the product of the density (ρ) and the sound speed (c) of the medium. This is the case in open water when the distance from the source is longer than a few acoustic wavelengths. However, there are situations where the relationship between particle velocity and sound pressure is not constant and where the particle motion may be relatively higher and therefore more important than the sound pressure. This is the case when the distance from the source is short and the acoustic wave front is spherical rather than plane. Unusual large particle motions can also occur by seismic interface waves propagating at the interface between water and bottom or at layers deeper in the bottom. These interface waves are excited by low frequency sources close the bottom and propagate along the water-bottom interface creating relative large horizontal and vertical particle movements. In the acoustic and seismic literature, these waves are referred to as Rayleigh, Stoneley and Scholte waves, or simply called ground roll waves.

To this author's knowledge of the importance of interface waves have not been recognized and discussed in detail in relation to impact on marine life, with the exception of the paper by Hazelwood and Macey (2013), which inspired this study. The purpose in this short article is to discuss the excitation and propagation of transversal waves propagating along an interface between water and a solid medium, also (somewhat misleading) referred as an elastic medium. In order to account for this effect the complete wave theory for acoustic and seismic waves in layered media is needed. This theory can be found in text books, for instance Jensen et al. (2011) and Hovem (2010).

2 Theory on sound propagation over a solid bottom

The situation under consideration is depicted in Figure 1. A point source is located a height z_s above the sea floor and the receiving point is at a horizontal distance r at a height z above the bottom. The sea bottom may be composed of any number of layers. modeled as either fluid or solid layers with densities ρ_n, sound speeds c_{pn}, and shear speeds c_{sn}, where $n = 1,2,..., N$ for the layers in the bottom.

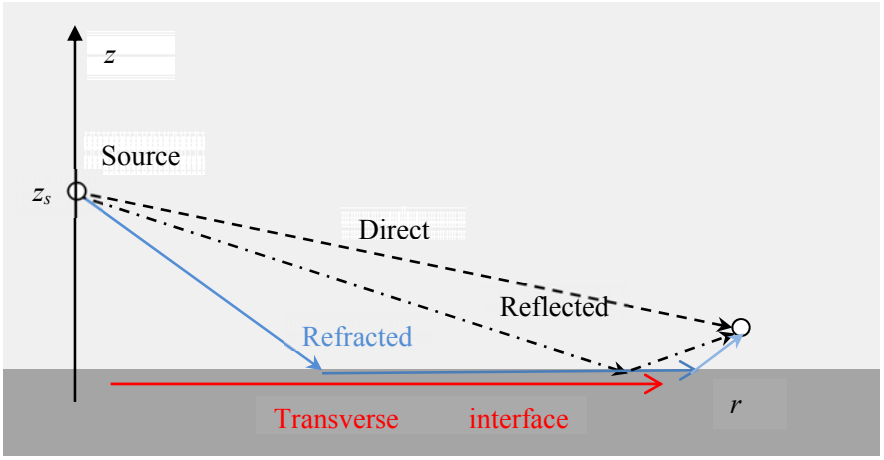

Figure 1. A point source, located at height z_s above a solid sea floor, and a receiver at height z and horizontal distance r from the source.

The signals reaching the receiver have several components, a direct and a bottom reflected signal, both indicated with dashed lines in the figure. Then there is a refracted signal, indicated by a solid blue line, entering the bottom at critical angel, propagating along the interface and radiates up to the receiving points. These waves exist also with a soft fluid-like bottom with no rigidity that cannot support shear waves. With a solid bottom, defined as a bottom that can support shear waves, there will be additional wave components, a transversal waves propagating along the interfaces at speeds somewhat lower than the shear speeds of the seafloor. Interface waves are excited by sources close to the bottom and may only be received at receivers close to the bottom. Interface waves of this type have particle displacements in the sagittal plane with a horizontal and vertical components decaying exponentially with distance from the interface, both in the water and in the bottom. Since many researches are of the opinion that that fish is more sensitive to particle

velocity than to the sound pressure, it is important that potential effects of interface waves should be taken into account.

Following the treatment and the notation of Hovem (2010, the received signal $\phi(r,z,\omega)$ with angular frequency ω at depth z, range r is expressed by an integral over the horizontal wave numbers

$$\begin{aligned}\phi(r,z,\omega) = &\frac{S(\omega)}{4\pi i}\int_0^\infty \frac{\exp\left(i\gamma_0|z-z_s|\right)}{\gamma_0} kJ_0(kr)\,dk \\ &+\frac{S(\omega)}{8\pi i}\int_0^\infty R_b(k)\frac{\exp\left(i\gamma_0|z+z_s|\right)}{\gamma_0} kH_0^{(1)}(kr)\,dk\end{aligned} \tag{1}$$

In this expression $J_0(kr)$ the 0-order Bessel function of first kind and $H_0^{(1)}(kr)$ is the 0-order Hankel function of the first kind representing an outgoing cylindrical wave. $S(\omega)$ is the frequency function of the source signal. The vertical wave number component in the water is γ_0, and the horizontal wave number component is k. These components are related frequency and the sound speed in the water c_0 by

$$\gamma_0 = \sqrt{\left(\frac{\omega}{c_0}\right)^2 - k^2} \tag{2}$$

The phase velocity v is related to the angular frequency ω and the horizontal wave number k by

$$v = \frac{\omega}{k} \tag{3}$$

The first term in equation (1) is the direct signal from the source, and the second term is the signal reflected from the medium below. The reflectivity of the seafloor, defined by the plane wave reflection coefficient $R_b(k)$, is a function of the incident angle expressed by the horizontal wave number component k. The reflection coefficient contains all reflections including the multiple reflections from underlying layers for both compressional waves and shear waves.

When $\phi(r,z,\omega)$ denotes the velocity potential the normal stress, equal to negative pressure is

$$\sigma = -\rho\frac{\partial}{\partial t}\phi(r,z,\omega) = i\omega\rho\phi(r,z,\omega) \tag{4}$$

The vertical u_z and the horizontal particle velocities u_r are given by

$$\begin{aligned}u_z &= \frac{\partial}{\partial z}\phi(r,z,\omega) \\ u_r &= \frac{\partial}{\partial r}\phi(r,z,\omega)\end{aligned} \tag{5}$$

The numerical solutions of these equations are obtained by using the wavenumber integration technique Jensen et al. (2011), which is implemented in the OASES model, Schmidt (1987, 2004). This model is used to generate synthetic signals for different cases, but first the some aspects of the physics are considered by simple examples. Note that in this discussion possible horizontally polarized waves are neglected since these are not excited by a point source.

3 An example with a point source over a solid half space

Consider the situation depicted in Figure 1, but with only one elastic layer having compressional wave speed c_{p1}, shear speed c_{s1} and density ρ_1. The sound speed in the water is c_0 and the density is ρ_0. In the following the emphasis is on the second term in equation (1) with the bottom-interacting component,

$$\phi_b(r,z,\omega) = \frac{S(\omega)}{8\pi i}\int_0^\infty R_b(k)\frac{\exp\left(i\gamma_0|z+z_s|\right)}{\gamma_0}kH_0^{(1)}(kr)\,dk \tag{6}$$

This expression for the reflected signal can for long ranges can be simplified by replacing the Hankel function with the asymptotic expression that applies to distances much greater than the acoustic wavelength. The reflected signal $\phi_R(r,z,\omega)$ is then with good approximation given as

$$\phi_R(r,z,\omega) = \frac{S(\omega)\exp(-i\pi/4)}{4\pi\sqrt{2\pi r}}\int_0^\infty R_b(k)\frac{\sqrt{k}}{i\gamma_0}\exp\left(i\gamma_0|z+z_s|+ikr\right)dk \tag{7}$$

Equations (6) or (7) show that the response will have at least two major contributions, when $R_b(k)$ is very large and when the vertical wave number γ_0=0. The maximum values of $R_b(k)$ can be found numerically and it turns out that in most cases the maximum values occurs when

$$k \approx \frac{\omega}{c_s} \tag{8}$$

The corresponding phase velocity is therefore approximately equal to the shear wave speed of the upper strata of the bottom. A more detailed analysis shows that phase velocity is a little less, about 95%, of the shear speed. With the value of equation (8)inserted in equation (2) it is evident that the vertical wave number in the water γ_0 is imaginary. When $c_{s1} < c_0$, as often is the case, and also assume here, the vertical wave number component in the water γ_0 approximately attains the value of

$$\gamma_0 \approx i\frac{\omega}{c_{s1}} \tag{9}$$

From equations (6) or (7) it follows that the depth dependence of the interface wave is determined by the exponential term and the amplitude is therefore proportional to,

$$a(z) \propto \exp\left(-\frac{\omega}{c_{s1}} |z + z_s| \right) \tag{10}$$

A shear- wave skin depth can be defined as

$$\delta_{shear} = \frac{c_{s1}}{\omega} = \frac{1}{2\pi} \lambda_{shear} \tag{11}$$

where λ_{shear} is the wavelength of the shear waves in the upper layer of the bottom. At a distance of $z = \delta_{shear}$ the amplitude is reduced to e^{-1}or by 8.69 dB relative to the amplitude at the surface of the bottom

The range dependence is determined by the Hankel function of equation (6) and the shear wave absorption, hence

$$\begin{aligned} a(r) &\propto H_0^{(1)}(kr) \\ k &= \frac{\omega}{c_s}(1 + i\beta) \end{aligned} \tag{12}$$

The imaginary component β of the wave number is related to the absorption coefficient α in Neper per wavelength by

$$\beta = \frac{\alpha}{2\pi} \tag{13}$$

Figure 2 shows a plot of the reduction in amplitude as function of range, according to equation (12), and height above bottom according to equation (10) calculated for the frequency of 50 Hz and value of β that corresponds to in 0.2 dB per shear wavelengths. Without absorption the amplitude of interface waves decay with $10\log_{10}$ (r) at long ranges, as seen from equation (7). In comparison, the amplitude of the direct wave decays with $20\log_{10}$ (r). In Figure 2 the geometrical decay of $10\log_{10}$ has been removed.

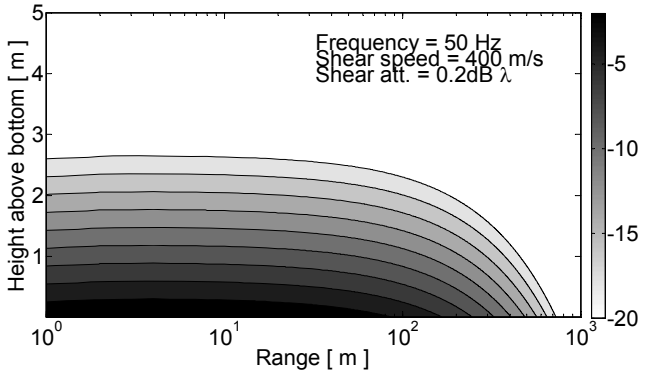

Figure 2. Normalized amplitude of a 50 Hz interface wave as function of range and combined height above bottom and for the shear speed and attenuation specified in the legend.

Equation (8) implies that a slow-propagating wave can exist at the interface between the water and the solid bottom, and that the speed of this interface wave is directly related to the shear speed of the bottom material.

In addition to the two wave components, there is a third wave contribution, the refracted wave. This wave is caused by the so-called stationary point in the integration of equation (7), see Hovem (2010). In the cases considered here, the refracted arrival is very week and are ignored, but can actually be observed in some of the simulated pulse plots shown later.

The reflected signal from the bottom is entirely determined by the reflection coefficient $R_b(k)$. The reflection coefficient at an interface between a fluid and a solid medium is

$$R_b = \frac{Z_{p1}\cos^2(2\theta_{s1}) + Z_{s1}\sin^2(2\theta_{s1}) - Z_0}{Z_{p1}\cos^2(2\theta_{s1}) + Z_{s1}\sin^2(2\theta_{s1}) + Z_0} \tag{14}$$

The impedances in equation (14) are

$$Z_0 = \omega\frac{\rho_0}{\gamma_0} \qquad Z_{p1} = \omega\frac{\rho_1}{\gamma_{p1}} \qquad Z_{s1} = \omega\frac{\rho_1}{\gamma_{s1}} \tag{15}$$

The angles are

$$\begin{aligned} \cos(2\theta_{s1}) &= 2\cos^2(\theta_{s1}) - 1 = 2\frac{k^2}{\omega^2}c_{s1}^2 - 1 \\ \sin(2\theta_{s1}) &= 2\sin(\theta_{s1})\cos\theta_{s1} = 2k\gamma_{s1}\frac{c_{s1}^2}{\omega^2} \end{aligned} \tag{16}$$

Figure 3 shows the reflection coefficient $R_b(k)$ calculated as a function of the horizontal wave number k for the parameters: frequency f = 5 Hz, c_0 = 1500 m/s, c_{p1} = 2000 m/s, c_{s1} = 400 m/s, ρ_0 = 1000 kg/m^3, and ρ_1=2000 kg/m^3. The attenuations of the compressional and the shear waves are both set to 0.2 dB per wavelength. According to equation (8) the peak at k=0.079 corresponds to a phase velocity of 395.7 m/s, which is a little less than the shear speed of 400 m/s.

Figure 4 shows a plot of the integrand of equation (6) for the same case and parameters as used to generate Figure 3. The red dotted line mark the location of the poles of the interface wave, the green dotted line marks the direct and the reflected arrivals and the dotted black line is the refracted wave. The three straight lines give the velocities of the various wave components according to equation (3). In For instance at the frequency of 100 Hz three wave components have peaks for the values of k equal to 1.59, 0,42 and 0.315 corresponding to phase velocities 395 m/s, 1500 m/s and 2000 m/s for the interface wave, the reflected wave, and the refracted waves respectively. The fact that the peaks are on straight lines means that the waves propagate with constant velocities independent of frequency and therefore the waves are not dispersive. Notice that the green line, the line for the sound speed in the water, gives the limit for real incident angles. This means that interface waves are not excited by plane wave incident, but by spherical waves as a near field effect. Hence propagation models that describe the bottom interaction with plane wave reflection

coefficients, such as described in Hovem and Korakas (2013) and Korakas and Korakes (2013), cannot adequately account for interface waves. In most cases, this may not be important for the acoustic field in the water, but may be a serious deficiency for the calculation of the acoustic field near the bottom.

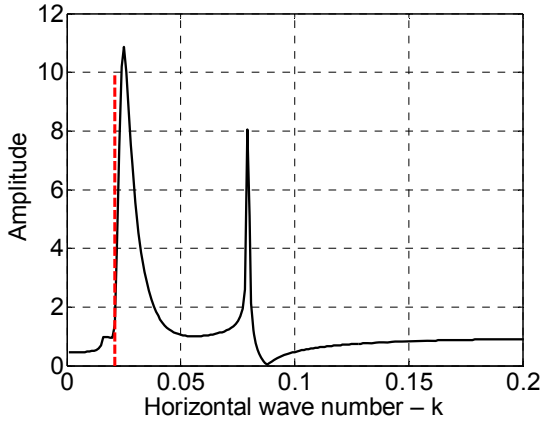

Figure 3. Absolute value of the reflection coefficient of a homogeneous elastic medium as a function of the horizontal wave number. The frequency is 25 Hz and the parameters of the bottom are given in the text. The red dotted line gives the upper limit of k for real incident angles.

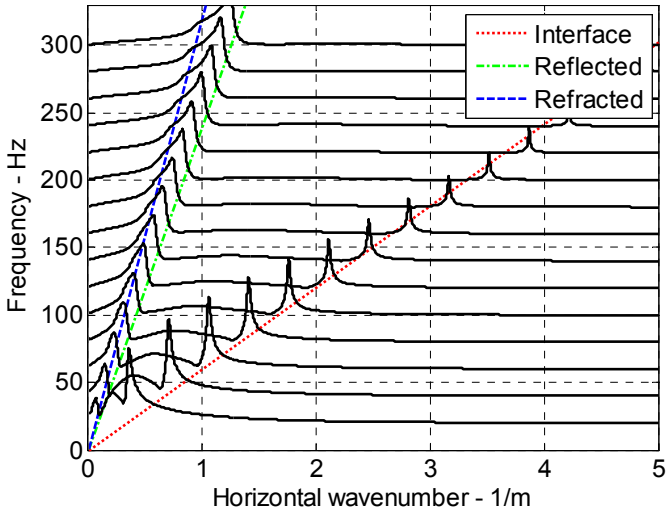

Figure 4. Absolute value of the integrand of (6) for a homogeneous elastic bottom as function of the horizontal wave number and frequency. The straight lines indicate the contribution of the interface waves and the reflected and refracted waves as given in the legend.

4 Case studies using the OASES model

The OASES model, Schmidt (1987, 2004), is used to illustrate how the sound pressure and the particle velocities may vary with frequency and with the seismo-acoustic properties of the bottom.

In the first case the water depth is 100 m and the bottom is assumed to be a homogenous solid half-space with density ρ_1=2000 kg/m^3, compressional wave speed c_{p1} = 2000 m/s, shear speed c_{s1} = 400 m/s. The attenuations of both the compressional and the shear waves in the bottom are 0.2 dB /wavelength. The source pulse is a 5 Hz Ricker source pulse with pulse shape and frequency spectrum shown in Figure 5 and the source depth is 95 m, 1 m above the bottom.

Figure 6 shows the received pulses at different ranges of for the normal stress component (left), the vertical (middle) and the horizontal particle velocity (right). The very first, almost invisible, arrivals are the refracted waves arriving just before the strong direct and the bottom reflected pulses. The last arrivals are the slow interface pulses present in all components, but relatively stronger in the vertical component. In these plots, compensation for spherical spreading has been applied by proportionally increasing the amplitudes with range. Therefore, the amplitudes of the direct and reflected pulse shapes appear to be constant with range.

The pulse responses in Figure 6, where shear wave conversion is included, is compared with pulse responses in Figure 7 computed when shear waves are ignored by setting shear speed c_{s1} equal to zero. Figure 7 shows that now the interface arrivals disappear, but the all other arrivals are unchanged.

The next case is with a layered bottom with 20 m layer over a solid half-space. The parameters of the upper layer are the same as used to generate Figure 6, but the solid half-space has ρ_2=2200 kg/m^3, compressional wave speed c_{p2} = 2200 m/s, and shear speed c_{s2} = 600 m/s, the attenuations of both the compressional and the shear waves in the bottom are 0.2 dB per wavelength.Figure 8 shows that the main difference in comparison with Figure 7Figure 6 is that the interface waves are spread out in time. This time dispersion is caused by the depth dependence of the shear speed from 400 m/s at the surface of the bottom to 600 m/s at 20m depth into the bottom. The lowest frequency components of source signal penetrate deeper than the higher frequency components such that the lower frequency arrive earlier then the higher components. The spread in arrival times of the interfaces waves corresponds to the variation of shear speed from about 600 m/s to 400 m/s.

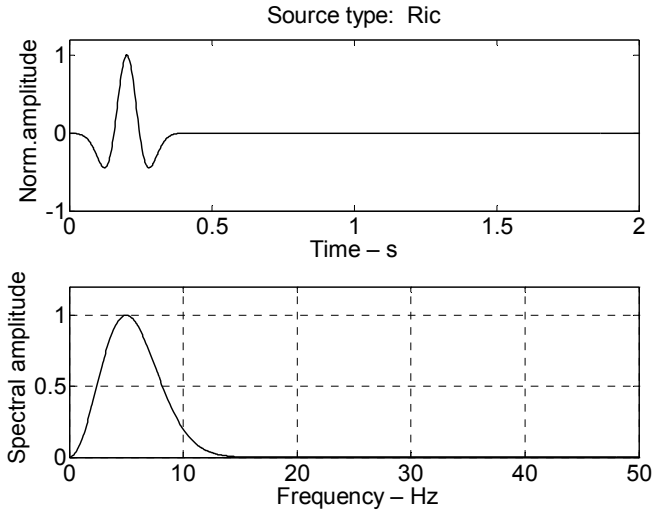

Figure 5. Ricker source pulse (5 Hz) and its frequency spectrum

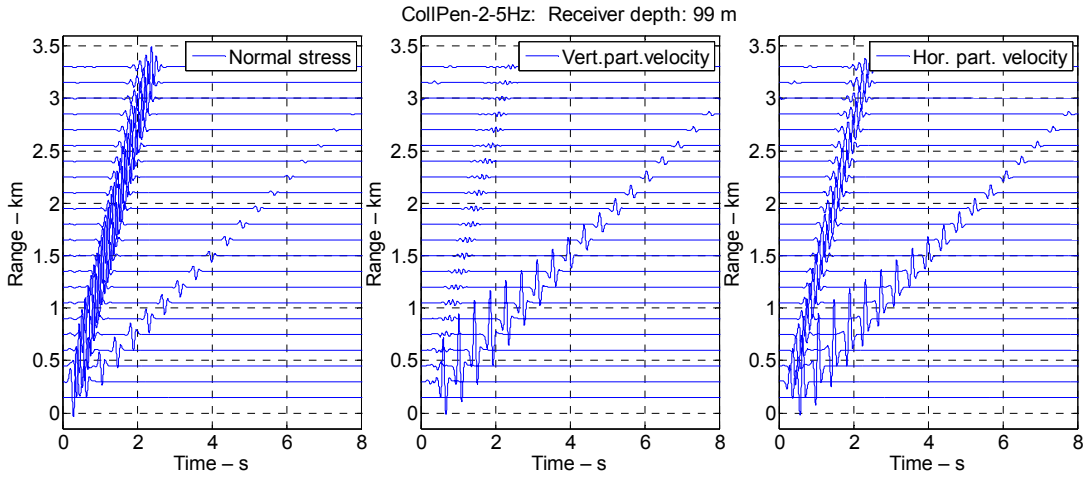

Figure 6. Pulse responses over a homogenous elastic bottom at depth of 100 m. Normal stress, vertical particle velocity, and horizontal particle velocity as function of range from the source. The source depth is 95m (5 m above the bottom) and receiver at 99 m (1 m above the bottom).

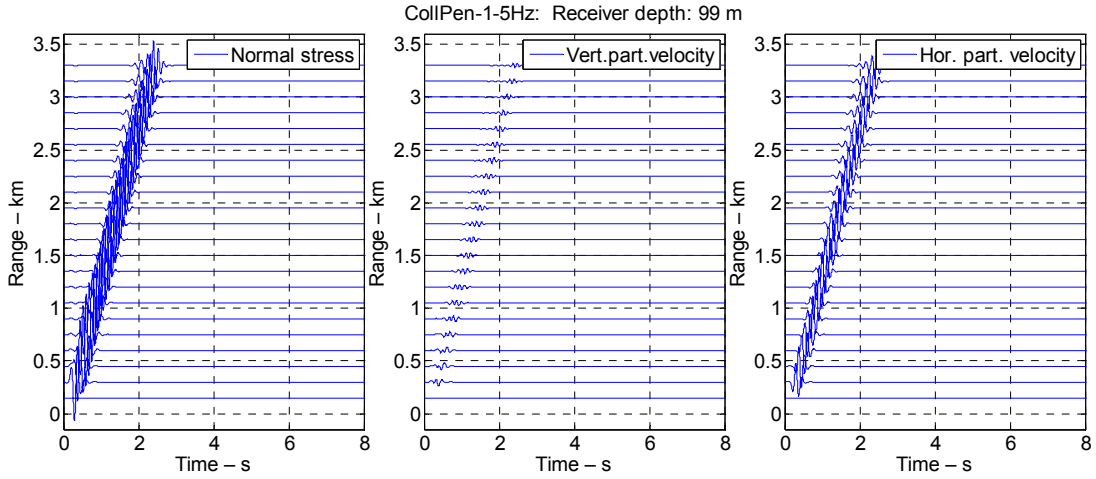

Figure 7. Pulse responses over a fluid bottom at depth of 100m. Normal stress, vertical particle velocity, and horizontal particle velocity as function of range from the source. The source depth is 95m (5 m above the bottom) and receiver at 99 m (1 m above the bottom).

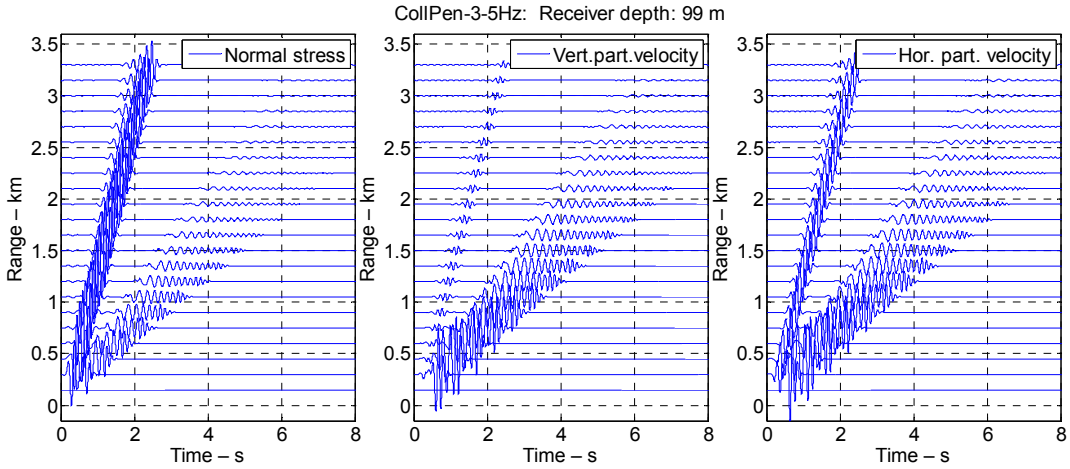

Figure 8. Pulse responses over a layered elastic bottom at depth of 100 m. Normal stress, vertical particle velocity, and horizontal particle velocity as function of range from the source. The source depth is 95m (5 m above the bottom) and receiver at 99 m (1 m above the bottom).

Whereas the previous examples are for the very low frequency of 5 Hz, the last example considers the frequency of 50 Hz, which may be more relevant for fish. The source pulse has the same shape as before (Figure 5), but compressed in time with a factor of 10 and the spectrum now peaks at 50 Hz. The bottom is layered as before, but the thickness of the upper layer is reduced to 5 m to illustrate the dispersion effect.Figure 9 shows the pulse shapes for the normal stress and the two components of the particle motions for distances up to 500 m. The interface wave contributions are quite significant in all components, most significant for vertical particle velocity. In this case, the skin depth is 1-2 m and the range extension, from Figure 2, is about 400-500 m.

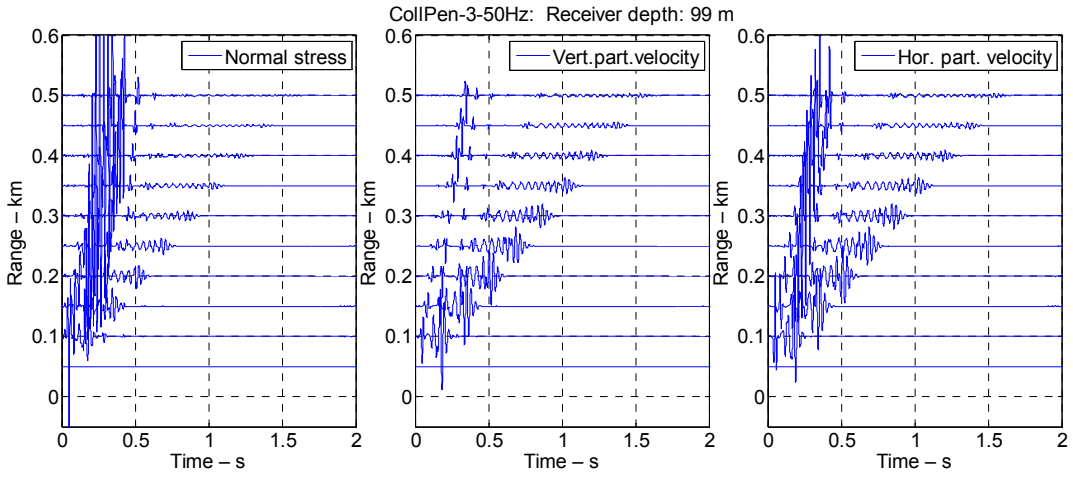

Figure 9. Pulse responses over a layered elastic bottom at depth of 100 m. Normal stress, vertical particle velocity, and horizontal particle velocity as function of range from the source. The source depth is 98m (2 m above the bottom) and receiver at 99 m (1 m above the bottom).

5 Summary and conclusions

The purpose of this article is to discuss the particle motions of seismic interface waves generated by low frequency sources close to solid rigid bottoms propagating along an interface between water and a solid elastic medium. Seismic interface waves are transversal waves in the sagittal plane with significant particle motions, particularly in the vertical component. The amplitude of the interface waves decays exponentially with distance from the bottom and may therefore have effect on marine life on the bottom or very close to the bottom. The strength and propagation of interface waves are dependent on the seismo-acoustic properties of the bottom, particularly the shear speed and attenuations of the bottom. The values of these parameters are not easy to find and therefore it is difficult to find in the literature, but some values are given in Hamilton (1987).

In this paper, the basic theory is outlined and the OASES propagation model is used to study how the sound pressure and the particle velocities of interface waves may vary with frequency and with the seismo-acoustic properties of the bottom.

Particle motion sensitivity may be important for fish responding to low frequency anthropogenic such as sounds generated by piling and explosions. At present, very little work has been carried out on the sensitivity of fish and other organisms, including marine invertebrates, to particle motion. It is therefore recommended that future experiments be conducted with three-axis vector sensors in addition to hydrophones to monitor the full acoustic field.

6 Acknowledgement

This work is part of the CollPen project of the Institute of Marine Research and financed by The Norwegian Research Council (Grant 204229/F20)

7 References

Hamilton, E. L. 1987. Properties of sediments. In *Acoustics and ocean bottom*, A. Lara-Sáenz, C. Ranz-Guerre, and C. Carbó-Fité, eds. II F. A. S. E. Specialized Conference, Madrid, June.

Hazelwood, Dick., Patrick Pacey, "*Ground roll waveforms in saturated sediments- generation by piling or by explosion*", Proceeding of the 1st Underwater Acoustics Conference and Exhibition, 23rd to 28th June 2013, Corfu Island, Greece. ISBN 987-618-80725-0-3, pp. 179-184.

Hovem, Jens M and Alexios Korakas, (2013) "*Modelling low frequency propagation loss in the o*ceans". Proceeding of the 1st Underwater Acoustics Conference and Exhibition, 23rd to 28th June 2013, Corfu Island, Greece. ISBN 987-618-80725-0-3, pp. 1517-1522.

Hovem, Jens M, (2010) "Marine Acoustics – The Physics of Sound in Marine Environment", Peninsula Publishing, Los Altos, CA, USA. 650 pp.

Hovem, Jens M. and Alexios Korakas, (2013). "Modeling low frequency anthropogenic noise in the in the oceans - a comparison of propagation models" Submitted for publication in the special issue of the Marine Technology Society Journal focused on Maritime Technologies in Norway. October 2013

Jensen, Finn B., W. A. Kuperman, M. B. Porter, and H. Schmidt. (2011) Computational Ocean Acoustics, 2nd Ed., Springer, 794 pp.

Korakas, Alexios and Jens Martin Hovem (2013). Comparison of modeling approaches to low- frequency noise propagation in the ocean, Ocean 2013 MTS/IEEE Bergen, June 10-13, 2013

Popper, A. N. and Hastings, M.C. (2009). "The effects of anthropogenic sources of sound on fishes". J. Fish Biol. Vol.75. pp. 455–489.

Schmidt, H. (2004). OASES Version 3.1 User Guide and Reference Manual. Department of Ocean Engineering, Massachusetts Institute of Technology, Washington.

Schmidt, H., (1987). SAFARI: Seismo-acoustic fast field algorithm for range independent environments. User's guide, SR 113, SACLANT ASW Research Centre, La Spezia, Italy.

Tasker, M.L., Amundin, M., Andre, M., Hawkins, A., Lang, W., Merck, T., Scholik-Schlomer, A., Teilmann, J., Thomsen, F., Werner, S. and Zakharia, M. 2010. Marine Strategy Framework Directive Task Group 11 Report - Underwater noise and other forms of energy. Available from http://www.ices.dk/projects/MSFD/TG11final.pdf.